

## Phosphine Chemistry on Mo(110) and Oxidized Mo(110)

X. Zhang, A. Linsebigler, U. Heiz, and J. T. Yates, Jr.\*

Surface Science Center, Department of Chemistry, University of Pittsburgh, Pittsburgh, Pennsylvania 15260

Received: July 6, 1992; In Final Form: January 15, 1993

The adsorption and desorption of phosphine and the oxidation of phosphorus on Mo(110) and oxidized Mo(110) have been studied by using Auger electron spectroscopy (AES), temperature-programmed desorption (TPD), and low-energy electron diffraction (LEED). Both molecular desorption and dissociative processes were observed on Mo(110), leaving adsorbed P(a) species in a  $c(4 \times 1)$  overlayer structure. The P(a) species do not undergo diffusion into the bulk below 1000 K. On the oxidized Mo(110) surface, the phosphine adsorption and dissociation process was inhibited significantly. Phosphorus on the Mo(110) surface could be oxidized to produce PO(g) and PO<sub>2</sub>(g) species near 900 K, as detected by line-of-sight mass spectrometry; neither P<sub>2</sub>O<sub>3</sub>(g) nor P<sub>2</sub>O<sub>5</sub>(g) was observed.

### I. Introduction

Certain phosphorus compounds used in pesticides, herbicides, and chemical agents are extremely hazardous materials. Degradation of these chemicals into less harmful substances using heterogeneous catalytic methods is therefore of great importance.<sup>1</sup> The surface chemistry of phosphine and organophosphorus compounds has been studied on both single-crystal metals and semiconductors<sup>2-4</sup> and on supported metal catalysts<sup>5</sup> and oxides.<sup>6-8</sup> The decomposition and oxidation of the organophosphorus compound dimethyl methylphosphonate on certain single-crystal surfaces, Ni(111),<sup>9</sup> Pd(111),<sup>9</sup> Mo(110),<sup>10</sup> and Pt(111),<sup>11</sup> have also been investigated. Studies on Mo(110) and Pd(111) showed that the rate-limiting surface process to establish a continuous oxidation reaction was the regeneration of catalytically active sites which were free of chemisorbed phosphorus. Phosphorus is removed by the production of volatile phosphorus oxides. On this basis, we have selected the catalytic oxidation of elemental phosphorus as a key issue for study. The oxidation of phosphine has also been studied recently on a supported MoO<sub>3</sub> catalyst.<sup>12</sup> Here, infrared spectroscopy was used to observe surface intermediates present in the oxidation process, and a final stage of phosphorus oxide desorption was observed at about 800 K.

As part of the continuing systematic comparative study of phosphorus oxidation on a variety of transition metals and oxides, this paper reports the study of the oxidation of elemental phosphorus on a Mo(110) single crystal and also on MoO<sub>x</sub> thin films prepared by adsorbing oxygen on Mo(110) at high temperature. A related study of the surface chemistry of phosphine on Mo(110) is also presented here.

### II. Experimental Section

The experiments were performed in a stainless steel ultrahigh-vacuum system described in detail previously.<sup>13</sup> The typical system base pressure was less than  $1 \times 10^{-10}$  mbar. The ultrahigh-vacuum chamber is equipped with a differentially pumped and digitized quadrupole mass spectrometer (QMS) for temperature-programmed desorption (TPD), a cylindrical mirror analyzer (CMA) for Auger electron spectroscopy (AES), low-energy electron diffraction (microchannel plate amplifier, LEED), and two calibrated and collimated capillary array dosers. The QMS was located in a differentially pumped shield containing a 1.6-mm-diameter aperture. This arrangement permits study of temperature-programmed desorption from the front face of the Mo(110) crystal by line-of-sight detection using the mass spectrometer.

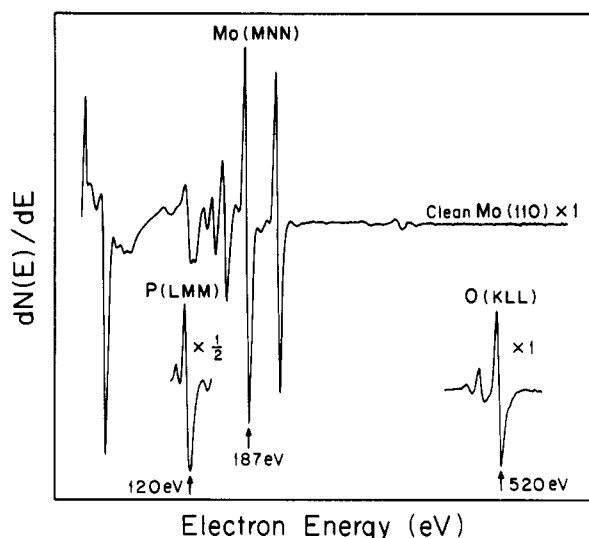


Figure 1. Auger spectrum of the clean Mo(110) single crystal. Also shown are the phosphorus Auger peak for saturated phosphorus on the surface and the oxygen peak for MoO<sub>x</sub> ( $y = \text{O}/\text{Mo}$  Auger ratio = 0.3).

The Mo(110) single crystal (12-mm diameter  $\times$  2-mm thickness) was polished with standard techniques and oriented within 1° of the (110) direction by Laue back-reflection X-ray diffraction. It had two 0.35-mm slots cut into the top and bottom for mounting. Resistive heating of the 0.35-mm-diameter tungsten wires held in the slots led to crystal heating by conduction. The crystal temperature was measured by a chromel-alumel thermocouple spot-welded to the back of the crystal. A linear heating rate (1.1 K/s) was achieved with an electronic temperature programmer.<sup>14</sup>

The initial crystal cleaning procedure is described elsewhere.<sup>10</sup> Each day the crystal was cleaned by cycles of oxygen treatment at 1100 K (carbon removed) and Ar<sup>+</sup> sputtering (1 keV, 1100 K) (O, P, and S removed) followed by annealing to 1200 K in vacuum.

These procedures produced a clean Mo(110) surface within the detection limit of AES, and a sharp (1  $\times$  1) LEED pattern was obtained after these procedures. The Auger spectrum of the clean Mo(110) is shown in Figure 1. The surface was considered to be free of sulfur when the [Mo + S](151 eV)/Mo(187 eV) ratio reached a steady value of 0.16 and was considered to be free of phosphorus when the [Mo + P](120 eV)/Mo(187 eV) ratio reached a steady value of 0.21. The values of the P(120 eV)/Mo(187 eV) ratio reported in this paper were obtained from the

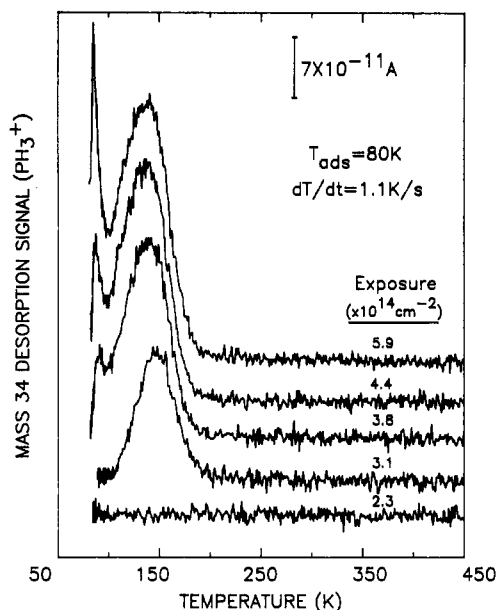


Figure 2. Temperature-programmed desorption spectra of  $\text{PH}_3$  on Mo(110) as a function of exposure.  $dT/dt = 1.1$  K/s.

difference between the measured  $[\text{Mo} + \text{P}](120 \text{ eV})/\text{Mo}(187 \text{ eV})$  value and 0.21.

Phosphine and deuterium gas were dosed to the crystal surface through a calibrated microcapillary array collimated beam doser.<sup>15-18</sup> The doser axis was oriented normal to the surface and delivered a flux of  $3.19 \times 10^{12} \text{ PH}_3/(\text{cm}^2 \text{ s})$  to the surface when the gas line pressure was 0.5 Torr. At the crystal position 12 mm from the doser, a geometrical interception factor of 0.3 was employed<sup>16,17</sup> to calculate the flux received by the crystal. In the phosphorus oxidation experiment, oxygen was delivered to the system through a leak valve to a steady system pressure in the  $10^{-8}$ – $10^{-5}$  mbar range while the crystal was positioned and heated in front of the QMS.

Phosphine was obtained from Matheson Gas Products (99.9% pure). Three freeze-pump-thaw cycles were performed before it was used. Deuterium was obtained from Cambridge Isotope Laboratories (D, 99.8% pure).

### III. Results

**Auger Spectroscopy Studies of P/Mo(110).** Figure 1 shows the Auger spectrum of a clean Mo(110) single crystal. Also shown are the  $P(LMM)$  peak after phosphine decomposition and the  $O(KLL)$  peak of  $\text{MoO}_x$  ( $O(520 \text{ eV})/\text{Mo}(187 \text{ eV})$  ratio  $y = 0.3$ ). It was found from P/Mo Auger ratios that the surface phosphorus did not diffuse into the Mo(110) crystal in the temperature range 600–1000 K. This result differs from studies on P/Pt(111)<sup>3a</sup> where surface phosphorus diffused into the bulk at 600–900 K. An analysis of the Auger intensity ratios suggests that an atom ratio P/Mo of about 0.4 exists in the depth of Auger sampling for the  $\text{PH}_3$  saturated surface. In addition, it was found that electron irradiation (3.0 kV,  $8 \times 10^{17} \text{ e}/\text{cm}^2$ ) did not result in perceptible loss of surface phosphorus by electron-stimulated desorption, indicating that Auger spectroscopy was not a perturbing probe for measurements of phosphorus surface coverage.

**Adsorption and Desorption of  $\text{PH}_3$ .** A series of TPD experiments were performed for different  $\text{PH}_3$  exposures at 80 K. Adsorbed phosphine was partially desorbed, and partially dissociated, producing P(a) and H(a). H(a) desorbed as  $\text{H}_2$ , and phosphorus was left on the surface of the crystal after heating. Figure 2 shows phosphine TPD spectra from the Mo(110) surface for increasing exposure to phosphine. At low exposures, there was no phosphine desorption. All of the phosphine decomposed completely either upon adsorption at 80 K or upon heating. At

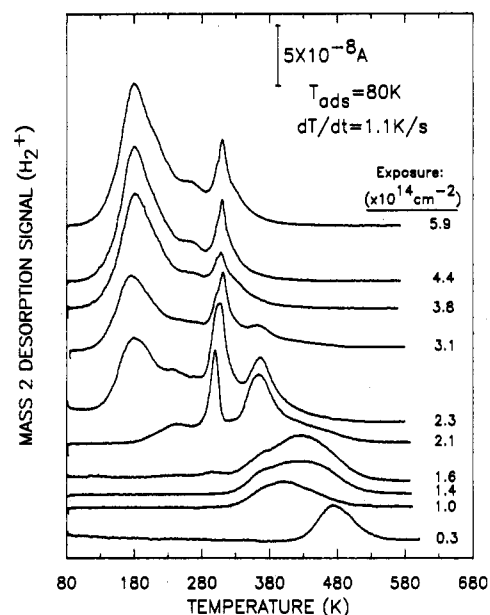


Figure 3. Temperature-programmed desorption spectra of  $\text{H}_2$  from dissociatively adsorbed  $\text{PH}_3$  on Mo(110) as a function of exposure.  $dT/dt = 1.1$  K/s.

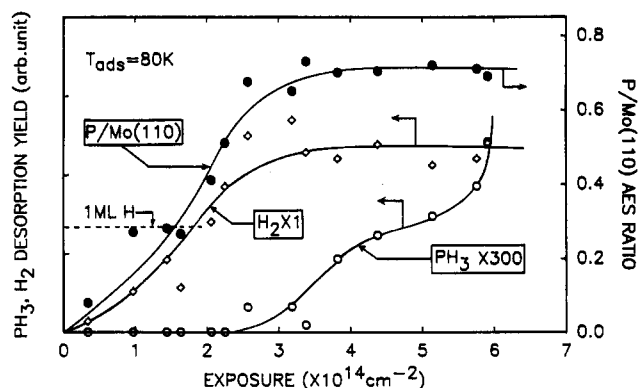


Figure 4.  $\text{PH}_3$  decomposition and desorption yields as a function of  $\text{PH}_3$  exposure. Desorption yields are calculated from total desorption peak areas. The saturation coverage of H was measured from  $\text{H}_2$  desorption from clean Mo(110) and is designated 1 ML in the figure.

intermediate exposures, only one phosphine desorption state was detected. This desorption state was due to the first layer of chemisorbed phosphine. At higher exposures, a low-temperature shoulder (85 K) developed; it originates from multilayer physisorbed phosphine.

Figure 3 shows a set of hydrogen desorption spectra from the TPD of dissociatively adsorbed  $\text{PH}_3$  on Mo(110) for increasing  $\text{PH}_3$  exposure. At low  $\text{PH}_3$  exposures, the hydrogen desorption behavior was similar to that for hydrogen desorption from clean Mo(110).<sup>19</sup> As the  $\text{PH}_3$  exposure was increased, two other low-temperature  $\text{H}_2$  desorption states developed. When the lowest-temperature  $\text{H}_2$  desorption state reached saturation, the maximum amount of phosphorus on the surface ( $\theta_{\text{P}}^{\text{rel}} = 1$ ) was obtained. Figure 3 also indicates that at higher coverages phosphine began to dissociate at a temperature of 120 K or lower, yielding hydrogen. The saturated hydrogen desorption yield from  $\text{PH}_3$  adsorption was  $1.77 \pm 0.06$  times greater than for pure hydrogen desorption from a hydrogen monolayer on clean Mo(110).

The effect of preadsorbed phosphorus on hydrogen adsorption on Mo(110) was studied at monolayer P coverage. Only the highest-temperature  $\text{H}_2$  desorption state was detected and amounted to 5% of the saturated coverage of hydrogen from  $\text{PH}_3$ .

Figure 4 shows the desorption yield of  $\text{H}_2$  and  $\text{PH}_3$  as a function of  $\text{PH}_3$  exposure. In addition, the buildup of the phosphorus

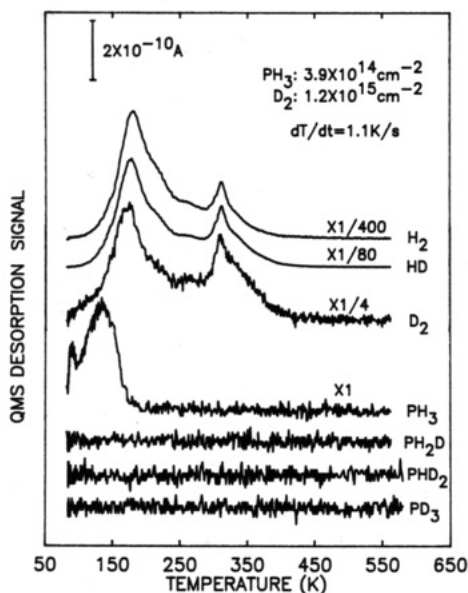


**Figure 5.** Temperature-programmed desorption spectra following deuterium and phosphine coadsorption on Mo(110). A mixture of deuterium and phosphine at the same gas line partial pressure was used.

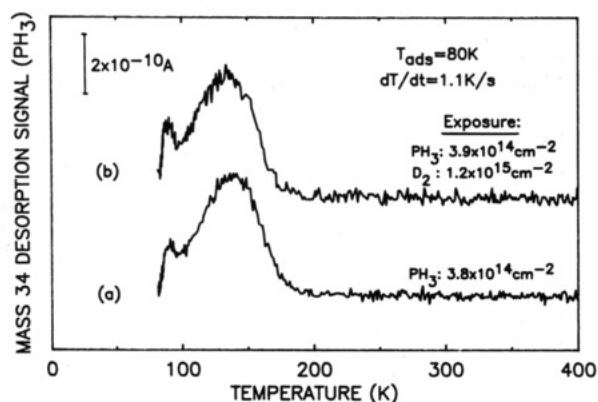


**Figure 6.** Comparison of  $\text{PH}_3$  TPD spectra from  $\text{PH}_3/\text{Mo}(110)$  and from  $\text{PH}_3/\text{D}_2/\text{Mo}(110)$ .

Auger signal for increasing  $\text{PH}_3$  exposures is shown. Auger spectra were taken after each TPD measurement. This figure indicates that at low exposures all of the phosphine is dissociated upon adsorption or heating. When the phosphine exposure is increased, the dissociation of  $\text{PH}_3$  reached saturation (at an exposure of about  $4 \times 10^{14} \text{ PH}_3 \text{ cm}^{-2}$ ), and additional adsorbed  $\text{PH}_3$  desorbs nondissociatively as  $\text{PH}_3$ . The three measurements conform to each other. Both the  $\text{H}_2$  desorption yield and the P/Mo Auger ratio reached saturation at an exposure to  $\text{PH}_3$  of about  $4 \times 10^{14} \text{ PH}_3 \text{ cm}^{-2}$ , and a little below this saturation exposure, phosphine began to desorb.

**Isotopic Exchange Studies.** To better understand phosphine adsorption and desorption on Mo(110), an isotope-exchange experiment was performed. Deuterium and phosphine at the same partial pressure were mixed in the gas line. Temperature-programmed desorption was carried out after the mixed gas was adsorbed on Mo(110) at 80 K. The result of this deuterium and phosphine coadsorption experiment is displayed in Figure 5. All the possible deuterium isotope-exchange products were monitored. For phosphine desorption, only  $\text{PH}_3$  was detected. Neither  $\text{PH}_2\text{D}$ ,  $\text{PHD}_2$ , nor  $\text{PD}_3$  was produced. For hydrogen desorption, all of the isotopically labeled hydrogen molecules were observed. This experiment indicates clearly that neither P(a) nor  $\text{PH}_x$ (a) recombines with D(a) to produce isotopically labeled phosphine molecules.

A comparison of phosphine desorption from  $\text{PH}_3/\text{Mo}(110)$  and from  $\text{PH}_3/\text{D}_2/\text{Mo}(110)$  was made, and the result is shown

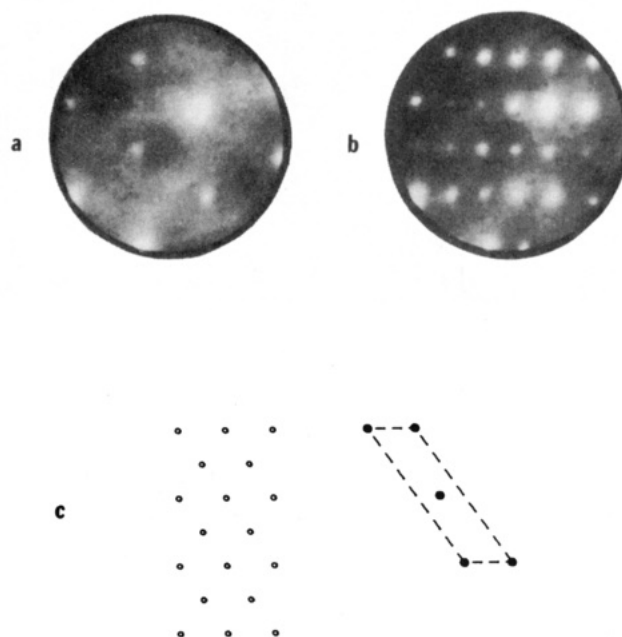


**Figure 7.** (a) LEED pattern of clean Mo(110). (b) LEED pattern of P/Mo(110). (c)  $c(4 \times 1)$  P overlayer structure compared to the unreconstructed Mo(110) surface. The P overlayer was produced from a saturated  $\text{PH}_3$  layer.

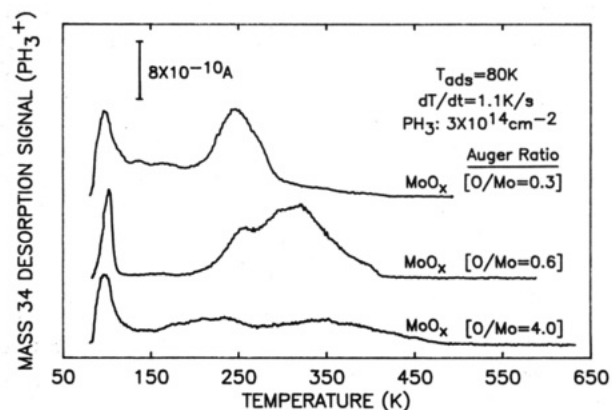


**Figure 8.** Temperature-programmed desorption spectra of  $\text{PH}_3$  on various  $\text{MoO}_x$  thin films. The  $y$  values,  $[\text{O}/\text{Mo}]$ , are O(520 eV)/Mo(187 eV) Auger peak-to-peak ratios.

in Figure 6. Coadsorbed deuterium had no effect on the phosphine desorption kinetics. In addition, the preadsorption of deuterium does not diminish the retention of P(a) from  $\text{PH}_3$  decomposition on Mo(110).

**LEED Studies of P/Mo(110).** LEED experiments were also performed. Adsorption of saturated  $\text{PH}_3$  at 80 K produced no extra LEED beams. After heating the crystal with saturated  $\text{PH}_3$  to 600–1000 K to leave only P(a) on the crystal, a  $c(4 \times 1)$  LEED pattern was observed. This indicates that phosphorus is ordered on Mo(110). Figure 7 shows the LEED patterns observed in these experiments and the phosphorus overlayer structure. A  $c(4 \times 1)$  structure corresponds to a coverage of 0.5 P atom/Mo atom.

**Adsorption and Desorption of Phosphine on  $\text{MoO}_x$ .** Molybdenum oxide layers were produced by exposing the Mo(110) crystal at 1000 K to  $\text{O}_2$ (g). Auger spectroscopy was used to measure the surface composition. One monolayer of molybdenum oxide was produced when the O/Mo(110) ratio was 0.3 ( $y = 0.3$ ).<sup>20</sup> An oriented oxide layer was produced when the O(520 eV)/Mo(187 eV) Auger ratio was 0.6 ( $y = 0.6$ ). A much thicker molybdenum oxide layer ( $y = 4.0$ ) was also prepared.

Temperature-programmed desorption spectra for  $\text{PH}_3$  from three different molybdenum oxide layers are shown in Figure 8.

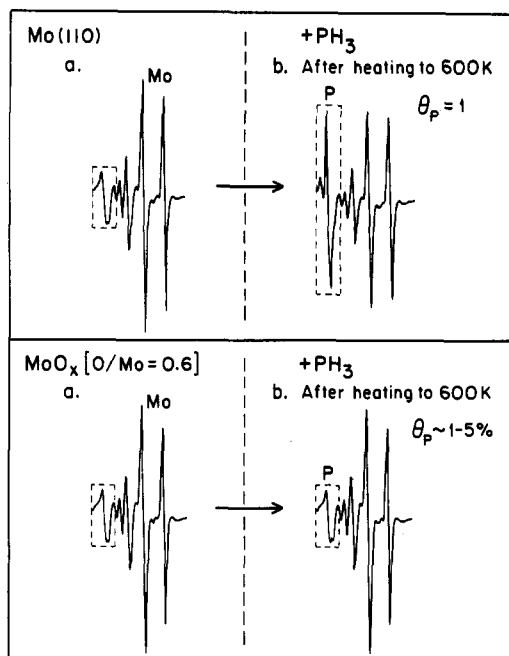


Figure 9. Auger spectra taken before phosphine adsorption and after phosphine desorption on Mo(110) and MoO<sub>x</sub> ( $y = 0.6$ ) thin film. The PH<sub>3</sub> exposure was  $3.8 \times 10^{14}$  PH<sub>3</sub>/cm<sup>2</sup>.

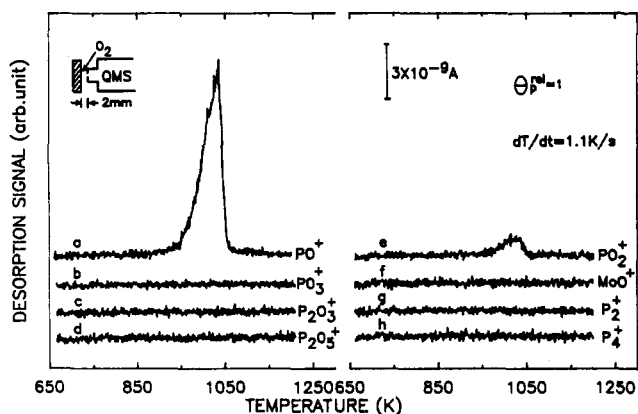


Figure 10. Phosphorus oxidation on Mo(110) in  $1.0 \times 10^{-5}$  mbar of O<sub>2</sub>. The masses monitored were (a) 47, (b) 79, (c) 110, (d) 142, (e) 63, (f) 112, (g) 62, and (h) 124 amu.

On all the MoO<sub>x</sub> layers, the phosphine decomposition was inhibited as was observed for phosphine on iron oxide.<sup>6a</sup> On one monolayer of MoO<sub>x</sub> ( $y = 0.3$ ), the phosphine decomposition is only 20% of that on Mo(110) as measured by the P/Mo Auger ratio taken after heating. In this case ( $y = 0.3$ ), besides phosphine, some hydrogen desorption was also detected. Only phosphine desorption was detected for the thicker molybdenum oxide layer. The chemisorbed PH<sub>3</sub> desorption maximum was shifted to higher temperatures (as the molybdenum oxide layer thickness increased) compared to phosphine desorption from Mo(110). The phosphine desorption kinetics were different on the different oxide layers as displayed in Figure 8.

The adsorption of phosphine on the oriented MoO<sub>x</sub> films ( $y = 0.6$  and  $y = 4.0$ ) was further investigated by Auger electron spectroscopy. Figure 9 shows the AES of Mo(110) and MoO<sub>x</sub> ( $y = 0.6$ ) taken before phosphine adsorption and after phosphine thermal desorption. After phosphine desorption, the phosphorus retained on the MoO<sub>x</sub> film was only 1–5% of that retained on Mo(110). This indicates that phosphine decomposition on the oriented molybdenum oxide layers was inhibited extensively below 600 K.

The desorption of H<sub>2</sub>O from PH<sub>3</sub>/MoO<sub>x</sub> layers was not detected by line-of-sight mass spectrometry.

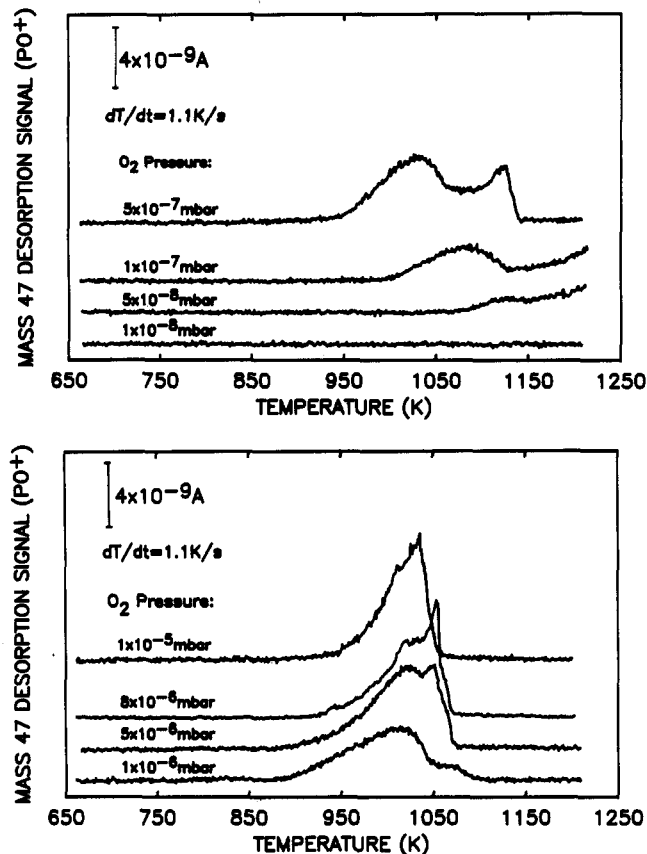


Figure 11. Phosphorus oxidation in an O<sub>2</sub> environment at different pressures. A saturated phosphorus layer was present on the surface. Oxygen was admitted to the chamber to the desired steady pressure.

**Phosphorus Oxidation on Mo(110) and MoO<sub>x</sub> ( $y = 0.3$ ).** Phosphorus oxidation experiments were performed by programmed heating of the crystal, containing a saturated phosphorus layer, in an oxygen background pressure while monitoring desorbed species from the surface by line-of-sight mass spectrometer measurements. Different oxygen pressures ( $1 \times 10^{-8}$  to  $1 \times 10^{-5}$  mbar) were used. MoO<sup>+</sup>, P<sub>2</sub><sup>+</sup>, P<sub>4</sub><sup>+</sup> and several kinds of phosphorus oxides were monitored. Only PO<sup>+</sup> and PO<sub>2</sub><sup>+</sup> were detected near 1050 K as shown in Figure 10. Because PO<sub>3</sub><sup>+</sup>, P<sub>2</sub>O<sub>3</sub><sup>+</sup>, and P<sub>2</sub>O<sub>5</sub><sup>+</sup> were not detected, the desorption species could only be PO and/or PO<sub>2</sub> according to the phosphorus oxides' cracking patterns.<sup>21</sup> The desorption products are designated as PO<sub>x</sub>.

A detailed study of phosphorus oxidation was carried out at various oxygen pressures. Phosphorus on the surface was converted to volatile oxides by temperature programming, and the desorption spectra yielding PO<sup>+</sup> in the mass spectrometer are shown in Figure 11. From the spectra, a trend could be seen indicating that phosphorus on Mo(110) could be removed from the surface completely by oxidation if the surface temperature was high enough. During the experiments the Mo(110) crystal was heated up to 1210 K, and at oxygen pressures higher than  $5 \times 10^{-7}$  mbar, phosphorus was removed completely. Auger spectra indicated that there was no phosphorus left on the surface after these oxidation procedures. The phosphorus oxide yields (monitored as PO<sup>+</sup>) as a function of steady-state oxygen pressure are plotted in Figure 12. Here two PO<sub>x</sub> desorption measurements at lower oxygen pressures are incomplete, as indicated by arrows, since some PO<sub>x</sub> species desorb above 1210 K.

The TPD spectra in Figure 11 indicate that there are two PO<sub>x</sub> desorption processes. Both processes shift to lower temperature when the O<sub>2</sub> pressure is increased from  $1 \times 10^{-8}$  to  $1 \times 10^{-6}$  mbar. The lowest onset temperature for PO<sub>x</sub> desorption from the Mo(110) single crystal was 900 K in  $1 \times 10^{-6}$  mbar of oxygen.

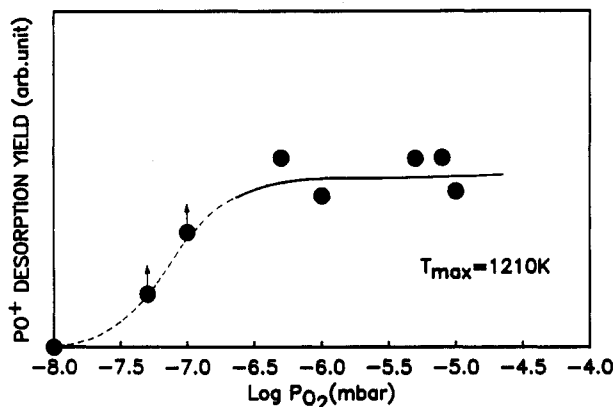


Figure 12.  $\text{PO}^+$  desorption yield as a function of oxygen pressure. The Mo(110) crystal was heated to 1210 K.

#### IV. Discussion

**Phosphine Adsorption on Mo(110): Coverage Estimations.** The basis for an estimation of the absolute saturation phosphine coverage on Mo(110) is related to the measured yield of hydrogen from the decomposed  $\text{PH}_3$ . Estimations of the saturation coverage of pure hydrogen on Mo(110) range from  $0.86 \times 10^{15}$  to  $1.73 \times 10^{15} \text{ cm}^{-2}$ .<sup>22</sup> It is noted that this upper limit for hydrogen absolute coverage corresponds to 1.2 H/Mo and is probably unrealistic.

We measured that the ratio of hydrogen evolution from a saturated  $\text{PH}_3$  layer to pure hydrogen (saturated) is  $1.77 \pm 0.06$ . This implies that the  $\text{PH}_3$  saturation coverage is in the range  $0.51 \times 10^{15}$  to  $1.02 \times 10^{15} \text{ cm}^{-2}$ . Therefore, based on the hydrogen yield from saturated  $\text{PH}_3$ , the phosphorus coverage ranges from 0.36 P/Mo to 0.73 P/Mo, using a Mo atom surface density of  $1.4 \times 10^{15} \text{ cm}^{-2}$  in the unreconstructed Mo(110) surface.

The  $c(4 \times 1)$  LEED pattern obtained for the P overlayer produced from the saturated  $\text{PH}_3$  corresponds to 0.5 P/Mo, well within the large range of the saturated absolute P coverage, based on  $\text{H}_2$  yield measurements.

From Figure 4, it may be seen that an exposure of about  $4 \times 10^{14} \text{ PH}_3/\text{cm}^2$  leads to  $\text{PH}_3$  saturation as judged by the yield of the hydrogen. This agrees fairly well with the lower estimate of the  $\text{PH}_3$  saturation coverage (about  $5 \times 10^{14} \text{ PH}_3 \text{ cm}^{-2}$ ) and is consistent with the lower estimate of the saturation coverage of pure hydrogen on Mo(110)<sup>22,23</sup> and also approximately with the LEED measurement ( $0.7 \times 10^{15} \text{ P/cm}^2$ ).

**Phosphine Bonding to Mo(110).** The bond between phosphine and a metal can be compared to that between CO and a metal. The phosphorus lone pair electrons act as an electron pair donor to Mo acceptor atoms, enabling the phosphorus atom in  $\text{PH}_3$  to adopt a pseudotetrahedral configuration on atop Mo sites. In addition to acting as a  $\sigma$  donor, however, phosphine can act as a  $\pi$  electron acceptor when vacant 3d orbitals of phosphorus interact with nonbonding orbitals of a transition metal, thus increasing the metal–P bond strength. By analogy to  $\text{PH}_3$  bonding in organometallic compounds,  $\text{PH}_3$  binding to atop Mo(110) sites is assumed. The above argument is traditional for  $\text{PH}_3$  bonding to a transition metal. It has been suggested recently that P–H  $\sigma^*$  orbitals participate in the  $\pi$  acceptor process for  $\text{PH}_3$  bonding.<sup>24</sup>

**Phosphine Desorption on Mo(110).** An analysis of the desorption kinetics of the high-temperature  $\text{PH}_3$  desorption state with peak maximum at 148 K (Figure 2) yields an extremely low activation energy and preexponential factor which is unrealistic for first-order desorption kinetics for  $\text{PH}_3$  with a coverage-independent heat of adsorption. A large half-width (about 44 K) for the  $\text{PH}_3$  desorption process is observed. In contrast, the sharp desorption feature at 84 K exhibits more normal desorption kinetics as judged by its small half-width, although the desorption kinetic order (zero or first order) cannot be determined from these data.

The unrealistic desorption kinetic behavior seen for the 148 K  $\text{PH}_3$  desorption process may be due to repulsive  $\text{PH}_3$ – $\text{PH}_3$  interactions in the overlayer, causing a significant coverage-dependent shift in the activation energy for desorption. Similar effects, due to repulsive dipole–dipole interactions, have been observed for  $\text{NH}_3$  on Ru(001).<sup>25</sup>

From the D(a) +  $\text{PH}_3$ (a) coadsorption experiment, coadsorbed deuterium had no effect on  $\text{PH}_3$  desorption, as shown in Figure 6, nor on the coverage of P(a) produced by  $\text{PH}_3$ (a) decomposition. This suggests that deuterium adsorbs on different sites from  $\text{PH}_3$ . Hydrogen is assumed to adsorb in the Mo(110) hollow sites, whereas  $\text{PH}_3$  is adsorbed on terminal sites of Mo(110). Also, from the deuterium isotope exchange experiment (Figure 5), we found that molecular phosphine desorption (about 148 K) did not occur via a recombination process, again suggesting that  $\text{PH}_3$ (a) and H(a) behave independently on Mo(110).

**$\text{PH}_3$  Adsorption on  $\text{MoO}_x$ .** A comparison between the thermal desorption results for  $\text{PH}_3$  on Mo(110) and  $\text{PH}_3$  on  $\text{MoO}_x$  (Figures 2 and 8) indicates that  $\text{MoO}_x$  surfaces result in the desorption of  $\text{PH}_3$  at higher temperatures than observed on Mo(110). Thus, the decomposition of  $\text{PH}_3$  is retarded by surface oxygen and/or the bond between  $\text{PH}_3$  and the surface is strengthened in the presence of surface oxygen. Figure 8 indicates that the bonding energy of  $\text{PH}_3$  to  $\text{MoO}_x$  increases somewhat as  $x$  increases, ultimately leading to a broad  $\text{PH}_3$  desorption state with the TPD peak maximum near 350 K.

**Volatile Oxidation Products from  $\text{PH}_3$  on Mo(110) and  $\text{MoO}_x$ .** Only  $\text{PO}^+$  and  $\text{PO}_2^+$  are detected by the line-of-sight mass spectrometer during the catalytic oxidation of  $\text{PH}_3$  (Figures 10–12). Because neither  $\text{P}_2\text{O}_3$  nor  $\text{P}_2\text{O}_5$  was detected, the volatile phosphorus oxide can only be  $\text{PO}_2$ (g) or a mixture of  $\text{PO}_2$ (g) and  $\text{PO}$ (g). The  $\text{P}_2\text{O}_3$  or  $\text{P}_2\text{O}_5$  mass spectrometer cracking pattern in ref 21 suggests that large relative intensities of  $\text{P}_2\text{O}_5^+$  and/or  $\text{P}_2\text{O}_3^+$  would have been detected if the neutral parent phosphorus oxide molecules were desorbed in this experiment. Both  $\text{PO}$ (g) and  $\text{PO}_2$ (g) are known molecules which are stable, and their thermodynamic properties have been evaluated from their spectra.<sup>26</sup>

#### V. Summary and Conclusions

The interaction of  $\text{PH}_3$  with Mo(110) and  $\text{MoO}_x$  films on Mo(110) has been studied in the temperature range 80–1210 K. The following results have been found.

1.  $\text{PH}_3$  adsorption on Mo(110) results in  $\text{H}_2$  desorption at temperatures near 120 K at the highest  $\text{PH}_3$  coverages. Thus, phosphine decomposition begins near or below 120 K on Mo(110), producing adsorbed P or  $\text{PH}_x$  species.
2. At high  $\text{PH}_3$  exposures, the presence of undecomposed chemisorbed  $\text{PH}_3$  was found on the basis of  $\text{PH}_3$  thermal desorption in two low-temperature  $\text{PH}_3$  desorption processes. Isotopic studies with D(a) +  $\text{PH}_3$ (a) indicate that neither exchange nor recombination reactions to produce  $\text{PH}_3$ (g) occur. In addition, preadsorbed deuterium does not diminish the capacity of Mo(110) to chemisorb  $\text{PH}_3$ .
3. No evidence for diffusion of adsorbed P into the Mo(110) bulk was obtained in the temperature range 600–1000 K.
4. The hydrogen thermal desorption was measured for various  $\text{PH}_3$  exposures. Higher  $\text{PH}_3$  coverages produce  $\text{H}_2$  desorption at temperatures below that for pure  $\text{H}_2$  desorption from Mo(110) as a result of a P(a)–H(a) repulsive interaction.
5. LEED studies of P/Mo(110) produced from the decomposition of a saturated  $\text{PH}_3$  layer show the production of a  $c(4 \times 1)$  overlayer, corresponding to 0.5 P/Mo. Studies of  $\text{H}_2$  desorption from  $\text{PH}_3$  and of the P/Mo Auger intensity indicate a saturation coverage range of  $\text{PH}_3$  corresponding to 0.36–0.73 P/Mo, where only the decomposed  $\text{PH}_3$  is measured in this case.
6. Phosphine dissociation on  $\text{MoO}_x$  films was inhibited compared to dissociation on the clean Mo(110). For a three-

dimensional MoO<sub>x</sub> layer, only 1–5% of the P/Mo Auger ratio could be obtained by monolayer PH<sub>3</sub> decomposition compared to clean Mo(110). MoO<sub>x</sub> layers retain undissociated PH<sub>3</sub> up to 350 K, whereas PH<sub>3</sub> desorption from Mo(110) is completed below 200 K.

7. Both PO<sup>+</sup> and PO<sub>2</sub><sup>+</sup> mass spectral cracking products were observed near 900 K during phosphorus oxidation over Mo(110) in O<sub>2</sub>(g). Neither P<sub>2</sub>O<sub>3</sub> nor P<sub>2</sub>O<sub>5</sub> products are produced under the condition of this ultrahigh-vacuum experiment.

**Acknowledgment.** The authors gratefully acknowledge the financial support of the Army Research Office (Contract DAAL03-91-G-0323). Ueli Heiz acknowledges an Andrew Mellon Postdoctoral Fellowship from the University of Pittsburgh.

### References and Notes

- (1) Ekerdt, J. G.; Klabunde, K. J.; Shapley, J. R.; White, J. M.; Yates, J. T., Jr. *J. Phys. Chem.* **1988**, *92*, 6182.
- (2) (a) Hegde, R. I.; Tobin, J.; White, J. M. *J. Vac. Sci. Technol. A3* (2), **1985**, 339. (b) Greenlief, C. M.; Hedge, R. I.; White, J. M. *J. Phys. Chem.* **1985**, *89*, 5681. (c) Hegde, R. I.; White, J. M. *Surf. Sci.* **1985**, *157*, 17. (d) Hegde, R. I.; Greenlief, C. M.; White, J. M. *J. Phys. Chem.* **1985**, *89*, 2886.
- (3) (a) Mitchell, G. E.; Henderson, M. A.; White, J. M. *Surf. Sci.* **1987**, *191*, 425. (b) Henderson, M. A.; White, J. M. *J. Am. Chem. Soc.* **1988**, *110*, 6939. (c) Mitchell, G. E.; Henderson, M. A.; White, J. M. *J. Phys. Chem.* **1987**, *91*, 3808.
- (4) Chen, P. J.; Colaianni, M. L.; Wallace, R. M.; Yates, J. T., Jr. *Surf. Sci.* **1991**, *244*, 177.
- (5) (a) Lu, G.; Darwell, J. E.; Crowell, J. E. *J. Phys. Chem.* **1990**, *94*, 8326. (b) Lu, G.; Crowell, J. E. *J. Phys. Chem.* **1990**, *94*, 5644.
- (6) (a) Hegde, R. I.; White, J. M. *J. Phys. Chem.* **1986**, *90*, 2159. (b) Hegde, R. I.; White, J. M. *Surf. Sci.* **1981**, *10*.
- (7) Henderson, M. A.; Jin, T.; White, J. M. *J. Phys. Chem.* **1986**, *90*, 4607.
- (8) (a) Templeton, M. K.; Weinberg, W. H. *J. Am. Chem. Soc.* **1985**, *107*, 97. (b) *Ibid.* **1985**, *107*, 774.
- (9) Guo, X.; Yoshinobu, J.; Yates, J. T., Jr. *J. Phys. Chem.* **1990**, *94*, 6839.
- (10) Smentkowski, V. S.; Hagans, P.; Yates, J. T., Jr. *J. Phys. Chem.* **1988**, *92*, 6351.
- (11) Henderson, M. A.; White, J. M. *J. Am. Chem. Soc.* **1988**, *110*, 6939.
- (12) Paul, D. K.; Rao, L. F.; Yates, J. T., Jr. *J. Phys. Chem.* **1992**, *96*, 3446.
- (13) Gates, S. M.; Russell, J. N., Jr.; Yates, J. T., Sr. *Surf. Sci.* **1985**, *159*, 233.
- (14) Muha, R. J.; Gates, S. M.; Basu, P.; Yates, J. T., Jr. *Rev. Sci. Instrum.* **1985**, *56* (4), 613.
- (15) Bozack, M. J.; Muehlhoff, L.; Russell, J. N., Jr.; Choyke, W. J.; Yates, J. T., Jr. *J. Vac. Sci. Technol.* **1987**, *A5*, 1.
- (16) Campbell, C. T.; Valone, S. M. *J. Vac. Sci. Technol.* **1985**, *13*, 408.
- (17) Winkler, A.; Yates, J. T., Jr. *J. Vac. Sci. Technol.* **1988**, *A6* (5), 2929.
- (18) Smentkowski, V. S.; Yates, J. T., Jr. *J. Vac. Sci. Technol. A7* (6), **1989**, 3325.
- (19) Ernst-Vidalis, M.-L.; Kamaratos, M.; Papageorgopoulos, C. *Surf. Sci.* **1987**, *189/190*, 276.
- (20) Colaianni, M. L.; Chen, J. G.; Weinberg, W. H.; Yates, J. T., Jr. *Surf. Sci.* **1992**, *279*, 211.
- (21) Muenow, D. W.; Uy, O. M.; Margrave, J. L. *J. Inorg. Nucl. Chem.* **1970**, *32* (11), 3459.
- (22) Mahnig, M.; Schmidt, L. D. *Z. Phys. Chem. (Munich)* **1972**, *80*, 71. It should be pointed out that the estimation of absolute hydrogen coverage on Mo(110) and on related W single crystals is of poor accuracy. The saturation coverage of the primary standard (W(100)) is reported to be  $1.5 \times 10^{15}$  H/cm<sup>2</sup> by Tamm and Schmidt (Tamm, P.; Schmidt, L. D. *J. Chem. Phys.* **1971**, *54*, 4775). A second measurement by Madey (Madey, T. E. *Surf. Sci.* **1973**, *36*, 281) reports  $2.0 \times 10^{15}$  H/cm<sup>2</sup> on W(100). Tamm and Schmidt estimated that errors of a factor of 2 in saturation hydrogen coverage may exist in their comparison of different crystals with W(100). Thus, for Mo(110) the range of saturation hydrogen coverage is  $0.86 \times 10^{15}$  to  $1.73 \times 10^{15}$  H cm<sup>-2</sup>.
- (23) Tamm, P.; Schmidt, L. D. *J. Chem. Phys.* **1971**, *54*, 4775.
- (24) (a) Corbridge, D. E. C. *The Structural Chemistry of Phosphorus*; Elsevier Scientific Publishing: New York, 1974; p 6. (b) Xiao, S.-X.; Trogler, W. C.; Ellis, D. E.; Berkovitch-Yellin, Z. *J. Am. Chem. Soc.* **1983**, *105*, 7033. (c) Orpen, A. G.; Connelly, N. G. *J. Chem. Soc., Chem. Commun.* **1985**, 1310. (d) Orpen, A. G.; Connelly, N. G. *Organometallics* **1990**, *9*, 1206. (e) Marynick, D. S. *J. Am. Chem. Soc.* **1984**, *106*, 4064.
- (25) Benndorf, C.; Madey, T. E. *Surf. Sci.* **1983**, *135*, 164.
- (26) *J. Phys. Chem. Ref. Data* **1985**, *14* (Suppl. 1), 1642, 1670.